

Utilization of a Neutral Wire Filter Inductor in a Three-Leg Four-Wire Active Power Filter

Sami PETTERSSON, Mika SALO, Heikki TUUSA

Tampere University of Technology, Finland

Summary: Three-leg active power filter topology is the cost effective solution implementing a four-wire active power filter but it has some disadvantages compared to four-leg topology. The lack of a neutral wire filter inductor results in larger filter losses and therefore the efficiency of the topology is impaired. The neutral wire filter inductor is typically used with the four-leg four-wire active power filter topology and significantly reduces switching frequency current ripple. In this paper the suitability of a neutral wire filter inductor for the three-leg topology is studied. The performance of three-leg topology with a neutral wire filter inductor is studied through computer simulations and laboratory tests. The results indicate that the use of the neutral wire filter inductor clearly improves the performance of three-leg topology.

Keywords: four-wire system, power quality, vector control, control delay compensation, performance

1. INTRODUCTION

Three-phase four-wire power distribution systems are commonly used for powering residential, office and civic buildings. Most of the applications connected to four-wire systems are single-phase electrical devices that draw current containing a great deal of low-frequency harmonics. In addition, the use of single-phase loads causes many other undesirable effects, such as unbalanced supply phase currents and a neutral current in the neutral wire of the system. The harmonic currents may distort the supply voltages while a large neutral current may overload the neutral wire and the distribution transformer. [5]

Four-wire active power filters (APF) provide an efficient solution to improve the quality of supply in three-phase four-wire systems. The properties of a four-wire APF include suppression of harmonic current components, compensation of neutral current, balancing of supply phase currents and power factor correction.

Basically, there are two common four-wire APF topologies [1]. Both topologies are voltage source shunt four-wire APFs and their main circuits differ from each other mainly in the number of semiconductor devices. A three-leg topology is based on a conventional three-leg converter with six controllable switches. In this case, the neutral wire is connected directly to the midpoint of the dc-link. The main circuit of the three-leg topology is shown in Figure 1a. Subscripts l, s, f and n refer respectively to load, supply, APF and neutral wire.

The other topology is a four-leg topology, whose main circuit is shown in Figure 1b. The four-leg topology uses a four-leg converter with eight controllable switches, the neutral wire being connected to the fourth leg of the converter through a neutral wire filter inductor.

The obvious advantage of the three-leg topology over the four-leg topology is the smaller number of semiconductor devices. As a drawback, the three-leg topology requires higher voltage level in the dc-link than the four-leg topology. Normally, the maximum modulation index of a three-phase

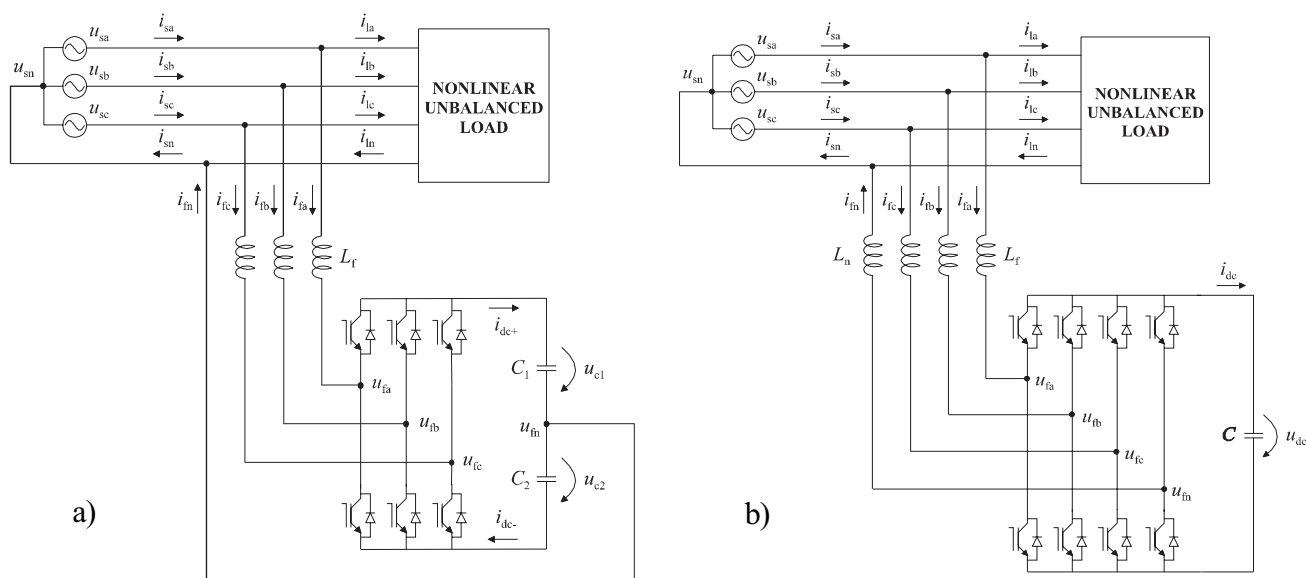


Fig. 1. Main circuits: (a) Three-leg topology. (b) Four-leg topology

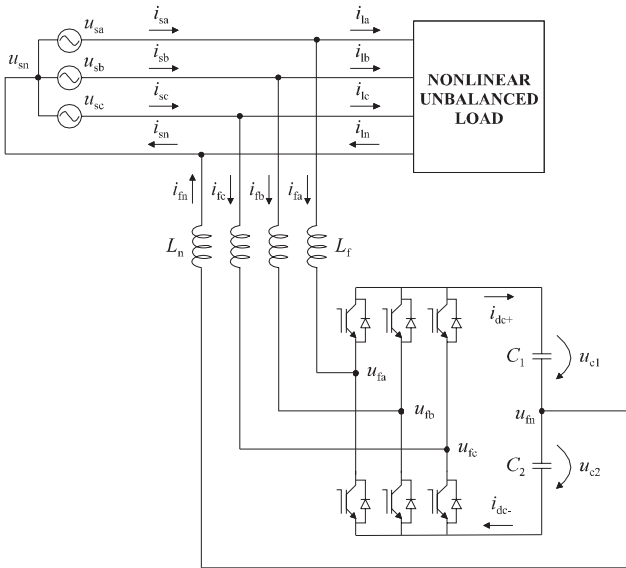


Fig. 2. Main circuit of a three-leg four-wire APF with a neutral wire filter inductor

voltage source PWM converter can be increased about 15 % by adding triplen harmonics to the voltage reference [2]. But the split-capacitor dc-link structure of the three-leg topology prevents the use of this method because the triplen harmonics would show in the neutral current. Thus, in theory, the three-leg topology requires 15% higher voltage in the dc-link than the four-leg topology in order to reach the same performance. Nevertheless, the simulation and experimental results show that the filtering performance of the low-frequency harmonics is approximately the same for both topologies when the level of dc-link voltage is adequate [4].

Even though the construction costs can be reduced by using fewer passive components in the main circuit, the lack of a neutral wire filter inductor can be considered the most significant disadvantage of the three-leg topology compared to the four-leg topology. Without the neutral wire filter inductor the suppression of the switching frequency current ripple in the neutral wire is insufficient, depending only on the phase line filter inductors. And since the resistance of an inductor typically increases as the frequency increases, larger switching frequency current ripple causes larger filter losses and the power dissipation of the APF increases. [4]

This paper presents a study of the suitability of the neutral wire filter inductor for the three-leg topology. The main circuit of the proposed topology is presented in Figure 2. The study is based on computer simulation and experimental results. The experiments were conducted in a laboratory with a microcontroller controlled four-wire APF prototype designed to be able to compensate the harmonics caused by a nonlinear and unbalanced load of 5 kVA nominal power. The experimental tests included filtering performance studies and power measurements.

2. NEUTRAL WIRE FILTER INDUCTOR

The effect of the neutral wire filter inductor on the neutral current can be studied by forming an equivalent circuit for the zero sequence current i_{fz} as shown in Figure 3 where R_f

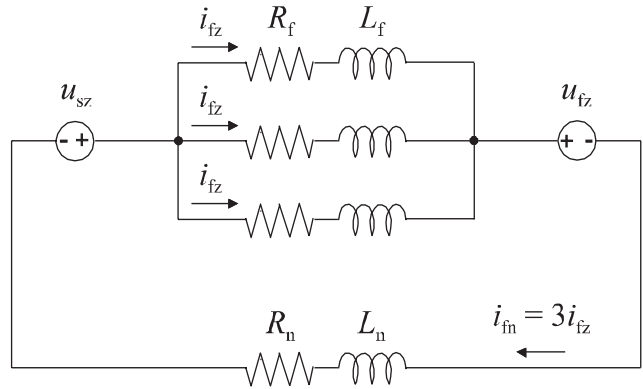


Fig. 3. Equivalent circuit for the zero sequence current

and L_f are the resistance and inductance of the phase line filter inductors respectively, R_n and L_n the resistance and inductance of the neutral wire filter inductor respectively, u_{sz} and u_{fz} the zero sequence voltage of the supply and APF respectively and i_{fn} the neutral current. In this case, the load is disconnected and therefore only the APF is connected to the supply.

A zero sequence component of three-phase quantities can be calculated as an average of the phase quantities [8]:

$$x_z = \frac{1}{3}(x_a + x_b + x_c) \quad (1)$$

where x is an arbitrary three-phase quantity. Since the neutral current is the sum of the phase currents, the relation between a zero sequence current component and a neutral current is [1]:

$$i_n = i_a + i_b + i_c = 3i_z \quad (2)$$

The idea of using the neutral wire filter inductor is to efficiently suppress the switching frequency current ripple on the neutral current generated by the APF. However, the inductance value of the neutral wire filter inductor should be selected so that the filter does not impair the controllability of the compensation neutral current flowing through the filter.

Now, on the basis of Figure 3, we can write the following equation:

$$u_{sz} - u_{fz} = \left(\frac{R_f}{3} + R_n \right) i_{fn} + \left(\frac{L_f}{3} + L_n \right) \frac{d}{dt} i_{fn} \quad (3)$$

As can be seen in (3), the inductance of the neutral wire filter inductor has a much more significant effect on the neutral current compared to the inductance of the phase line filter inductors. Therefore, the suppression of the switching frequency current ripple in the neutral wire can be considerably improved even with a neutral wire filter inductor of low inductance.

Next, the effect of the inductance value of the neutral wire filter inductor L_n on the system's performance at the filtering frequencies is considered. The neutral current of the APF i_{fn} depends on the zero sequence voltage u_{fz} generated by the APF, as can be seen in (3). Now, if the inductance L_n increases and the voltage u_{fz} is kept constant, the neutral current's

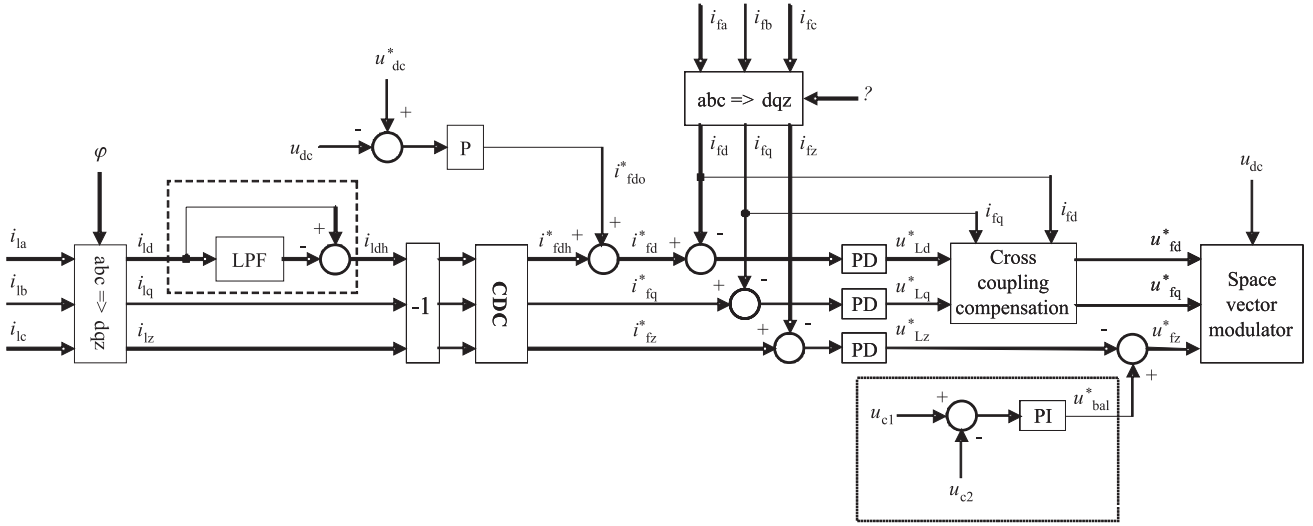


Fig. 4. Block diagram of the control system

rate of change decreases, which reduces the harmonic compensation performance of the system. Thus, the maximum generable zero sequence voltage u_{fz} defines the size of the inductor L_n that can be used.

Because of the smaller number of controllable switches in the main circuit of the three-leg topology the generable zero sequence voltage u_{fz} is significantly lower compared to the four-leg topology. This means that the size of the neutral wire filter inductor is much more limited in the case of the three-leg topology if the level of dc-link voltage is kept unchanged.

3. CONTROL SYSTEM

The control system of the APF is implemented in the synchronous reference frame where the real axis is tied to the supply voltage vector and therefore the fundamental currents appear as dc-components [3]. The block diagram of the control system is presented in Figure 4. Subscripts d and q denote real and imaginary axis components of a space vector in the synchronous reference frame. In addition, subscript h refers to harmonics, o to fundamental frequency quantities in the synchronous reference frame and z to a zero sequence component. An asterisk (*) refers to a reference value.

The control method is based on the load current feedforward connection. The task of the control system is to produce filter currents opposite to the harmonics sensed in the load currents. The neutral current is similarly compensated by producing a neutral current opposite to the neutral current caused by the load. The measured quantities required by the control system are the phase currents of the load (i_{la} , i_{lb} and i_{lc}) and APF (i_{fa} , i_{fb} and i_{fc}). Moreover, in order to maintain the desired dc-link voltage and voltage balance between the dc-link capacitors, the capacitor voltages u_{c1} and u_{c2} are also measured.

Before the control can be carried out, the measured load currents as well as the measured filter currents must be transformed into space vector form in the synchronous reference frame [4]. Because of this, the angle of the reference

frame φ is needed. This can be determined with a phase locked loop by observing the zero-crossing of phase-a supply voltage. The extraction of the harmonics is done with a high-pass filter. The high-pass filter is outlined with a broken line in Fig. 4. Only the d-component of the load current is high-pass filtered in order that the APF would compensate the fundamental reactive power drawn by the load.

The control system uses a computational control delay compensation (CDC) to reduce the effects of the control delay on the APF's performance [6–7]. The compensation method is based on the knowledge of the system dynamics of the APF: since the behavior of the filter current in case of step change in the current reference is known, the reference can be corrected so that the filter current behaves as desired. The algorithm can be written in discrete form as [6]:

$$i_{out}(k) = \frac{\tau_c}{T_s} [i_{in}(k) - i_{in}(k-1)] + i_{in}(k) \quad (4)$$

where i_{in} is the current component entering the CDC block, i_{out} the current component exiting the CDC block, τ_c the compensation time constant and T_s the sample time of the control system. The compensation is applied to every current component (i_{ldh} , i_{lqh} and i_{lz}).

In this paper the three-phase power supply is assumed to be ideal and balanced. Therefore, in the synchronous reference frame where the real axis is tied to the supply voltage vector, the zero sequence component u_{sz} and q-component u_{sq} of the supply voltage are zero. Thus, the instantaneous active power of the APF can be written as [8]:

$$p = \frac{3}{2} (u_{sd} i_{fd} + u_{sq} i_{fq}) + 3u_{sz} i_{fz} = \frac{3}{2} u_{sd} i_{fd} \quad (5)$$

Equation (5) shows that the active power of the APF can be controlled by simply acting on the d-component of the APF current i_{fd} . And the dc-link voltage of the APF can be controlled through the active power.

The dc-link voltage u_{dc} is controlled by using a P-controller. The voltage control loop gives a current reference

i_{fd}^* , which is added to the d-component of the harmonics i_{fdh}^* . This sum forms the d-component of the APF's current reference i_{fd}^* .

PD-controllers are used as the current controllers of the system. The outputs of the controllers are the voltage references of the filter inductor voltages u_{Ld}^* , u_{Lq}^* and u_{Lz}^* . The APF's voltage references u_{fd}^* and u_{fq}^* in the synchronous reference frame can be calculated as follows [3]:

$$u_{fd}^* = u_{sd} - u_{Ld}^* + \omega L_f i_{fq} \quad (6)$$

$$u_{fq}^* = -u_{Lq}^* - \omega L_f i_{fd} \quad (7)$$

where u_{sd} is the d-component of the supply voltage and ω the fundamental angular frequency. Equations (6) and (7) include the cross coupling compensation terms that are used for compensating the cross coupling between d- and q-components of the voltage reference vector u_f^* in the synchronous reference frame. These calculations are performed in the cross coupling compensation block in Figure 4.

Since the neutral wire is connected to the midpoint of the dc-link, the currents flowing through the dc-link capacitors are unequal and therefore the capacitor voltages are independent of each other. The dc-link voltage balance is maintained with a voltage balance controller. The voltage balance controller is outlined with a dotted line in Figure 4. The PI-controller gives the voltage reference u_{bal}^* that modifies the zero sequence component of the APF's voltage reference u_{fz}^* as follows:

$$u_{fz}^* = -u_{Lz}^* + u_{bal}^* \quad (8)$$

This forces the dc-link capacitor voltage balance to shift in the desired direction.

The modulation signals are generated using a space vector modulator. The theory of the modulation method is presented in [4].

4. SIMULATION AND EXPERIMENTAL RESULTS

The performance of the three-leg topology with and without the neutral wire filter inductor was studied through computer simulations and laboratory tests with a microcontroller controlled four-wire APF prototype. The simulations were done using Simulink® linked to SIMPLORER®. The control system was modeled with Simulink® and the main circuit with SIMPLORER®. The laboratory tests included power factor and power dissipation measurements in addition to filtering performance studies. The power factor measurements take into account the effects of distortion.

The prototype used in the laboratory tests was designed to compensate the harmonic currents produced by a nonlinear and unbalanced load of 5 kVA nominal power. The inductance of the neutral wire filter inductor was selected so that the APF's capability to suppress low-frequency harmonics did not significantly decrease with the fixed 750 V dc-link voltage.

Table 1. Parameters of the prototype

Supply phase-to-neutral voltage U_s	230 V
Supply frequency f_s	50 Hz
Phase line filter inductor L_f	5 mH
Neutral wire filter inductor L_n	1 mH
Dc-link capacitors C_1 & C_2	2.2 mF
Total dc-link capacitance C	1.1 mF
Modulation frequency f_{sw}	8 kHz
Dc-link voltage u_{dc}	750 V

Table 2. Load parameters

Total active power	4.2 kW
Power factor	0.92 cap
Smoothing inductor L_{smooth}	2.3 mH
Load inductor L_{load}	10 mH
Load capacitor C_{load}	40 μ F
Load resistor R_1	35.5 Ω
Load resistor R_2	64.2 Ω

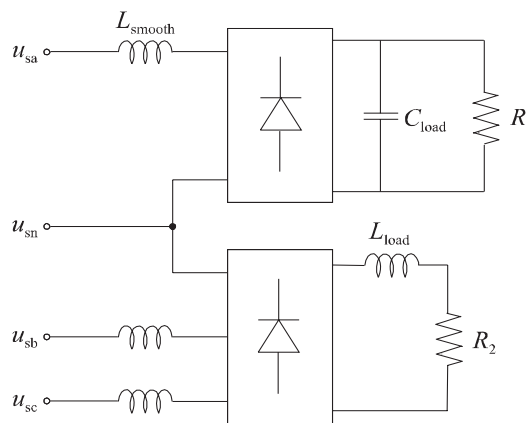


Fig. 5. Load

The parameters of the prototype are shown in Table 1.

The nonlinear and unbalanced load used in the simulations and in the experiments was created with two diode rectifier bridges as shown in Figure 5. The load parameters are shown in Table 2 and load current waveforms in Figure 6.

The simulated and measured supply current waveforms in the case of the three-leg APF without and with the neutral wire filter inductor are presented in Figure 7 and Figure 8 respectively. Fundamental components (I_1) and total harmonic distortion (THD) of the simulated and measured

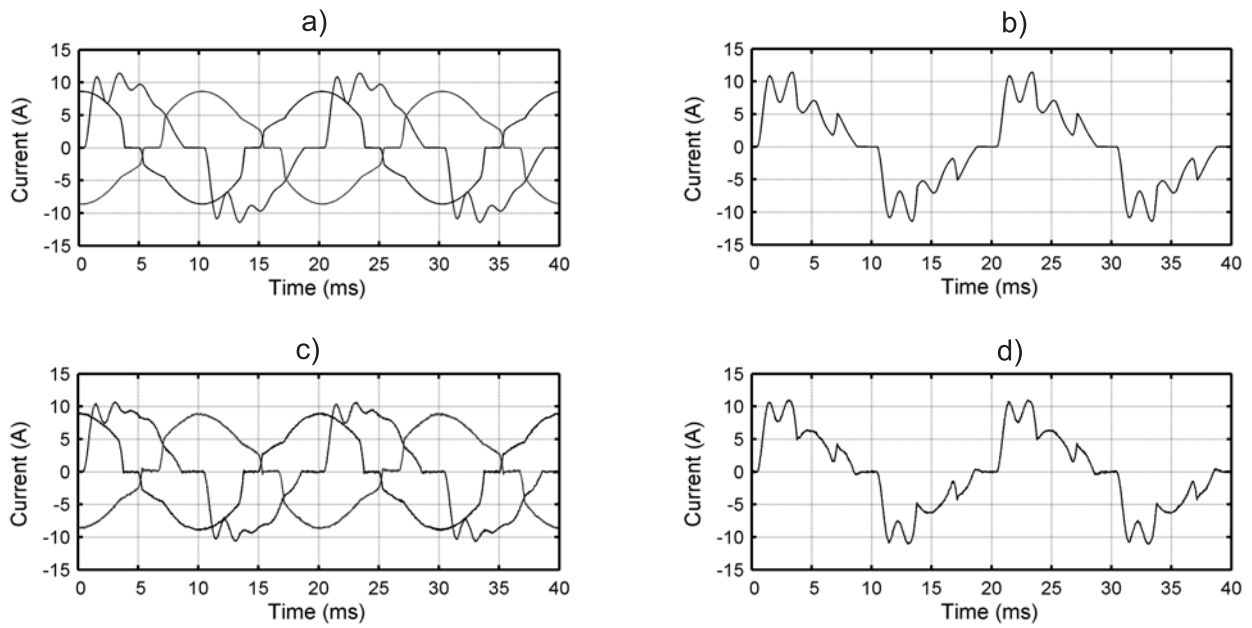


Fig. 6. Simulated and measured load current waveforms: (a) Simulated load phase currents. (b) Simulated load neutral current. (c) Measured load phase currents. (d) Measured load neutral current

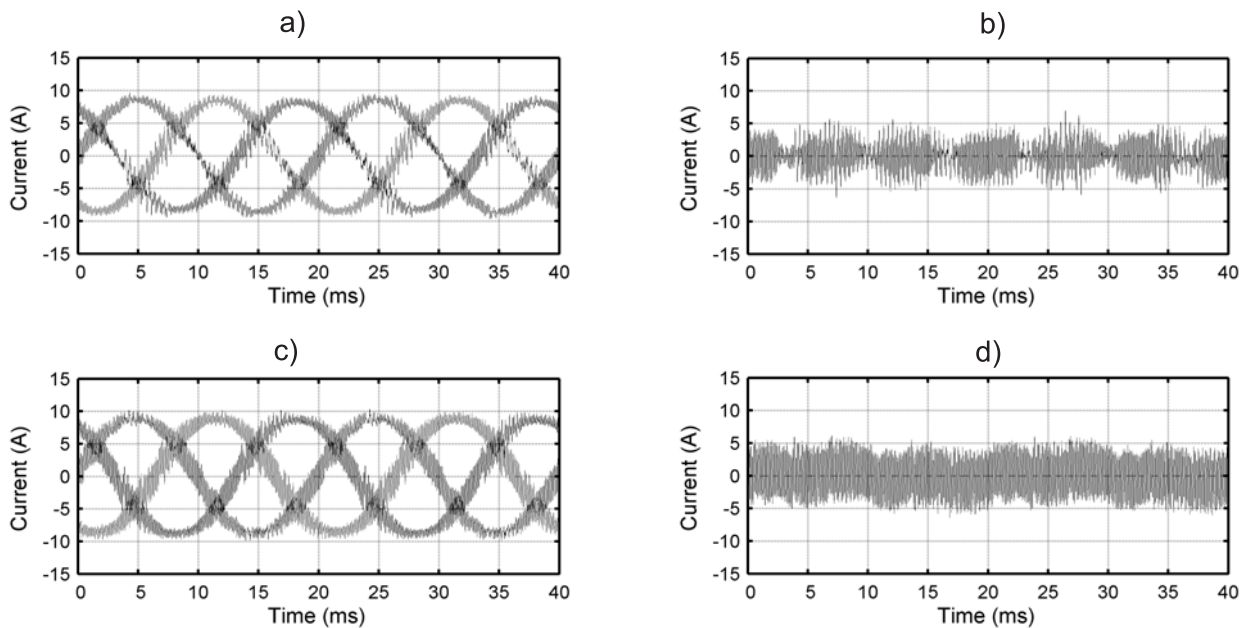


Fig. 7. Simulated and measured supply current waveforms in the case of the three-leg four-wire APF without the neutral wire filter inductor: (a) Simulated supply phase currents. (b) Simulated supply neutral current. (c) Measured supply phase currents. (d) Measured supply neutral current

waveforms are presented in Tables 3 and 4 respectively. In addition, Table 4 shows the results of power factor measurements.

The simulation and experimental results clearly indicate that the neutral wire filter inductor significantly reduces the amplitude of the switching frequency current ripple. In the simulations, the THD calculated up to 20 kHz was smaller than in the laboratory tests. The reason for this was that the inductors were modeled as a series connection of a resistor and an inductor. This kind of model does not take into

account the frequency dependence of the inductance and resistance that exists in reality. Therefore, the switching frequency current suppression was better in the simulations.

Table 4 shows that, in the laboratory tests, the THD calculated up to 20 kHz decreased approximately 27% with the neutral wire filter inductor, which is a significant improvement. The effect of the reduced switching frequency current ripple can also be seen in power measurements as lower power dissipation: the original three-leg APF dissipated 7.3% of the total power drawn from the mains and the three-leg APF with

Table 3. Fundamental components and THD of simulated waveforms

	Load		Three-leg APF		Three-leg APF with neutral wire filter inductor	
	i_{la}	i_{lc}	i_{sa}	i_{sc}	i_{sa}	i_{sc}
$I_1 (A_{rms})$	6.86	6.03	6.01	5.85	6.02	5.88
$THD_{2\text{ kHz}} (\%)$	23.98	12.95	2.56	3.58	2.60	3.61
$THD_{20\text{ kHz}} (\%)$			13.89	15.65	10.52	12.11

Table 4. Fundamental components, power factors and THD of measured waveforms

	Load		Three-leg APF		Three-leg APF with neutral wire filter inductor	
	i_{la}	i_{lc}	i_{sa}	i_{sc}	i_{sa}	i_{sc}
$I_1 (A_{rms})$	6.62	6.19	6.23	6.29	6.17	6.32
Power factor	0.93 cap	0.88 ind	0.98 cap	0.98 cap	0.99 cap	0.99 cap
$THD_{2\text{ kHz}} (\%)$	23.24	12.84	2.75	3.83	3.10	3.97
$THD_{20\text{ kHz}} (\%)$			17.78	18.22	12.99	13.22

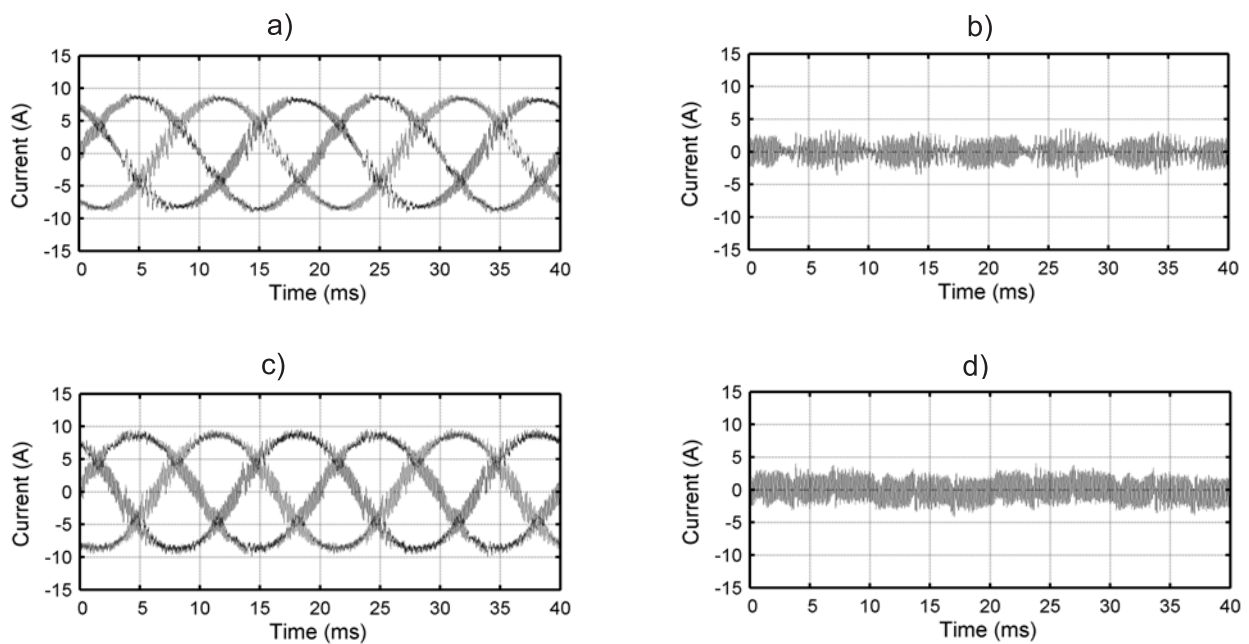


Fig. 8. Simulated and measured supply current waveforms in the case of the three-leg four-wire APF with the neutral wire filter inductor: (a) Simulated supply phase currents. (b) Simulated supply neutral current. (c) Measured supply phase currents. (d) Measured supply neutral current

the neutral wire filter inductor 6.3%. This means a 15% drop in power dissipation. Also, the power factor was slightly improved due to the reduced THD, as Table 4 indicates.

5. CONCLUSIONS

Insufficient suppression of switching frequency current ripple and resulting high power dissipation in the filter inductors are the most significant disadvantages of three-

leg four-wire APF topology compared to four-leg four-wire APF topology. The main reasons for this are the lack of a neutral wire filter inductor in the main circuit of the three-leg topology and higher dc-link voltage level.

In this paper the suitability of the neutral wire filter inductor for the three-leg four-wire APF topology was studied. The study was based on computer simulations and laboratory tests with a microcontroller controlled four-wire APF prototype. The inductance of the neutral wire filter inductor was selected so that the APF's capability to suppress low-

frequency harmonics did not significantly decrease.

The simulation and experimental results indicated that the use of the neutral wire filter inductor clearly improved the performance of the three-leg topology. Due to the reduced switching frequency current ripple, the power dissipation of the three-leg topology decreased by 15%.

However, the use of the neutral wire filter inductor is ultimately only a step in the right direction. The complete suppression of the switching frequency current ripple on the supply currents requires the use of more efficient passive filter structures.

REFERENCES

1. Fang-Zhuo, Yue-Wang and Zhao'an-Wang: *The configuration of main circuit and control strategy for active power filter in three-phase four-wire systems*. Power Electronics Specialists Conference – PESC 2001, 17th–21st June 2001, Vancouver, Canada, Vol. 3, pp. 1615–1618.
2. Holmes D.G. and Lipo T.A.: *Pulse Width Modulation for Power Converters – Principles and Practice*. Publisher: Wiley – Interscience, 2003, pp. 226–241.
3. Kim S. and Enjeti P.N.: *Control strategies for active power filter in three-phase four-wire systems*. Applied Power Electronics Conference and Exposition – APEC 2000, 6th–10th February 2000, New Orleans, Louisiana, USA, Vol. 1, pp. 420–426.
4. Pettersson S., Salo M. and Tuusa H.: *Performance comparison of the voltage source four-wire active power filter topologies*. International Power Electronics Conference – IPEC-Niigata 2005, 4th – 8th April 2005, Niigata, Japan, pp. 701–708.
5. Quinn C.A. and Mohan N.: *Active filtering of harmonic currents in three-phase four-wire systems with three-phase and single-phase non-linear loads*. Applied Power Electronics Conference and Exposition – APEC'92, 23rd–27th February 1992, Boston, Massachusetts, USA, pp. 829–836.
6. Routimo M., Salo M. and Tuusa H.: *A control delay compensation method for voltage source active power filter*. 9th European Power Quality Conference – PCIM 2003, 20th–22nd May 2003, Nürnberg, Germany, pp. 93–97.
7. Salo M. and Tuusa H.: *A novel open-loop control method for a current-source active power filter*. IEEE Transactions on Industrial Electronics, 50, 2, pp. 313–321, April 2003.
8. Vas P.: *Electrical Machines and Drives – A Space-Vector Theory Approach*. Publisher: Clarendon Press – Oxford, 1992, Chapter 2.



Sami Pettersson

was born in Hollola, Finland, in 1979. He received the M.Sc. degree in electrical engineering from Tampere University of Technology, Tampere, Finland, in 2004. Since 2004, he has been with the Department of Electrical Engineering, Tampere University of Technology, where he has been working as a Research Engineer. He is a Ph.D. student and his research interests are four-wire active power filters and their control methods.

Address:

Tampere University of Technology

Institute of Power Electronics

P.O. Box 692, FI-33101 Tampere, Finland

tel. +358 3 3115 2380, fax: +358 3 3115 2088,

e-mail: sami.pettersson@tut.fi



Mika Salo

was born in Pusula, Finland, in 1969. He received the M.Sc. (Eng.), Lic. Tech., and Dr. Tech. degrees in electrical engineering from Tampere University of Technology, Tampere, Finland, in 1996, 1998, and 2002, respectively. Since 1996, he has been with the Department of Electrical Engineering, Tampere University of Technology, where he was a Research Engineer in 1996, an Academic Assistant in 1997, a Senior Academic Assistant from 1998 to 2002, and since 2003, he has been a Senior Researcher. His research interests include power electronics and electrical machines and drives.

Address:

Tampere University of Technology

Institute of Power Electronics

P.O. Box 692, FI-33101 Tampere, Finland

tel. +358 3 3115 2148, fax: +358 3 3115 2088,

e-mail: mika.salo@tut.fi



Heikki Tuusa

was born in Hattula, Finland, in 1957. He received the M.Sc. (Eng.), Lic. Tech., and Dr. Tech. degrees in electrical engineering from Tampere University of Technology, Tampere, Finland, in 1982, 1987, and 1993, respectively. Since 1983, he has been with the Department of Electrical Engineering, Tampere University of Technology. He was a Laboratory Manager from 1983 to 1986 and in 1993, a Senior Academic Assistant from 1986 to 1992, an Acting Professor from 1994 to 1995, and an Associate Professor from 1995 to 1998. Since 1998, he has been a Professor and Head of the Institute of Power Electronics. His areas of interest are PWM converters and controlled motor drives.

Address:

Tampere University of Technology

Institute of Power Electronics

P.O. Box 692, FI-33101 Tampere, Finland

tel. +358 3 3115 2145, fax: +358 3 3115 2088,

e-mail: heikki.tuusa@tut.fi